The power threshold of H-mode access in mixed hydrogen–tritium and pure tritium plasmas at JET with ITER-like wall

G. Birkenmeier[1,2,*], E.R. Solano[3], E. Lerche[4], D. Taylor[5], D. Gallart[6], M.J. Mantsinen[6,7], E. Delabie[8], I.S. Carvalho[9], P. Carvalho[9], E. Pawelec[10], J.C. Hillesheim[5], F. Parra Diaz[11], C. Silva[9], S. Aleiferis[5], J. Bernardo[5,9], A. Boboc[5], D. Douai[12], E. Litherland-Smith[5], R. Henriques[9], K.K. Kirov[5], C.F. Maggi[5], J. Mailloux[12], M. Maslov[5], F.G. Rimini[5], S.A. Silburn[5], P. Sirén[5], H. Weisen[13] and JET Contributors[a]

[1] Max Planck Institute for Plasma Physics, Boltzmannstr. 2, 85748 Garching, Germany
[2] Physik-Department E28, Technische Universität München, James-Franck-Str. 1, 85748 Garching, Germany
[3] Laboratorio Nacional de Fusión, CIEMAT, Madrid, Spain
[4] Laboratory for Plasma Physics Koninklijke Militaire School, Ecole Royale Militaire Renaissancelaan 30 Avenue de la Renaissance B-1000, Brussels, Belgium
[5] CCFE, Culham Science Centre, Abingdon, Oxon OX14 3DB, United Kingdom of Great Britain and Northern Ireland
[6] Barcelona Supercomputing Center (BSC), Barcelona, Spain
[7] ICREA, Barcelona, Spain
[8] Oak Ridge National Laboratory, Oak Ridge, TN 37831-6169, TN, United States of America
[9] Instituto de Plasmas e Fusão Nuclear, Instituto Superior Técnico, Universidade de Lisboa, Portugal
[10] Institute of Physics, Opole University, Oleska 48, 45-052 Opole, Poland
[11] Rudolf Peierls Centre for Theoretical Physics, University of Oxford, Oxford OX1 3PU, United Kingdom of Great Britain and Northern Ireland
[12] CEA, IRFM, F-13108, St-Paul-Lez-Durance, France
[13] Ecole Polytechnique Federale de Lausanne (EPFL), Swiss Plasma Center (SPC), CH-1015 Lausanne, Switzerland

E-mail: gregor.birkenmeier@ipp.mpg.de

CrossMark

Abstract

The heating power to access the high confinement mode (H-mode), P_{LH}, scales approximately inversely with the isotope mass of the main ion plasma species as found in (protonic) hydrogen, deuterium and tritium plasmas in many fusion facilities over the last decades. In first dedicated L–H transition experiments at the Joint European Torus (JET) tokamak facility with the ITER-like wall (ILW), the power threshold, P_{LH}, was studied systematically in plasmas of pure tritium and hydrogen–tritium mixtures at a magnetic field of 1.8 T and a plasma current of 1.7 MA in order to assess whether this scaling still holds in a metallic wall device. The measured power thresholds, P_{LH}, in Ohmically heated tritium plasmas agree well with the expected isotope scaling for metallic walls and the lowest power threshold was found in Ohmic

---

* Author to whom any correspondence should be addressed.

phases at low density. The measured power thresholds in ion cyclotron heated plasmas of pure tritium or hydrogen–tritium mixtures are significantly higher than the expected isotope mass scaling due to higher radiation levels. However, when the radiated power is taken into account, the ion cyclotron heated plasmas exhibit similar power thresholds as a neutral beam heated plasma, and are close to the scaling. The tritium plasmas in this study tended to higher electron heating fractions and, when heated with ion cyclotron waves, to relatively higher radiation fractions compared to other isotopes potentially impeding access to sustained H-modes.

(Some figures may appear in colour only in the online journal)

1. Introduction

The high confinement regime (H-mode) is the most promising plasma regime for a tokamak fusion reactor with a positive triangularity and a medium aspect ratio and, therefore, the envisaged plasma scenario for ITER [1]. Although the detailed physics of the transition from L-mode to H-mode (L–H transition) is complicated and not quantitatively understood, experimentalists identified one major macroscopic control parameter to enter the H-mode: the total heating power of the plasma has to exceed a critical power, the L–H power threshold, P_{LH}. The L–H power threshold mainly depends on the magnetic field strength, the plasma density and the surface area of the last closed flux surface (LCFS) as found in the ITPA 2008 multi-machine scaling [2]

$$P_{scal} = 0.049\bar{n}^{0.72}B_t^{0.8}S^{0.94} \tag{1}$$

with the necessary power P_{scal} in MW, line-averaged core density $\bar{n}$ in units of 10^{20} m^{-3}, toroidal magnetic field B_t in T and surface area S of the LCFS in m^2.

This scaling does not reflect a well documented non-monotonic density dependence [3–8], the so called low density branch, since only data for higher densities were used for the scaling. The low density branch can appear below a certain density, $\bar{n}_{e,min}$, where P_{LH} is minimum. The P_{LH} curve above $\bar{n}_{e,\,min}$, i.e. for higher densities than $\bar{n}_{e,\,min}$, is referred to as the high density branch. The plasma current [9], the (effective) isotope mass of the main ions in the plasma [8, 10–13], the plasma shape [4, 14], the toroidal rotation [15], Z_{eff} [16], and further parameters [7, 17, 18] are additional factors determining P_{LH}.

For ITER, the actual value of P_{LH} has a major impact on the design of plasma scenarios, especially during the non-nuclear phase (PFPO-1), in which the available heating power is predicted to be only marginally above P_{LH} for hydrogen plasmas [19]. For a future DEMO reactor, if planned as a tokamak with positive triangularity and medium aspect ratio, P_{LH} directly determines the size of the device (major radius R). This is due to the interplay with the requirements for the heat exhaust, which poses a limit on the total power reaching the plasma boundary in order to stay below the material limits of plasma facing components, in connection with the known operational limits of a tokamak [20]. Thus, a reliable prediction of P_{LH}

especially for fusion-relevant isotope mixtures is required for any design of a classical tokamak reactor.

The majority of L–H transition studies addressing the isotope dependence of P_{LH} were done in H, He or D plasmas. All dedicated studies agree [8, 11, 13, 22], that P_{LH} is higher in H compared to D, typically by a factor of two indicating a mass scaling

$$P_{LH} \propto 1/A_{eff} \tag{2}$$

with the effective ion mass of the plasma

$$A_{eff} = \frac{n_H + 2n_D + 3n_T}{n_H + n_D + n_T} \tag{3}$$

with n_H the hydrogen ion density, n_D the deuterium ion density and n_T the tritium ion density.

Much less data is available for plasmas containing tritium, since tritium is expensive, difficult to handle due to its radioactive properties, and tritium plasma operation needs special safety licensing procedures. But also for tritium plasmas, the results, which were to date from plasmas in carbon wall devices only, suggest the same isotope dependence $P_{LH} \propto 1/A_{eff}$ [10]. The 2020/2021 tritium campaign at the Joint European Torus (JET) was one of the rare cases in the history of fusion research to study tritium plasmas and the first opportunity to get information on tritium containing plasmas in metallic wall conditions similar to ITER, i.e. a beryllium main chamber wall and a tungsten divertor.

The majority of the experiments presented were the very first pure tritium pulses after the last tritium campaign in 1997 and the start of the tritium campaign 2020/2021 in JET. *Pure tritium plasmas* in this context are plasmas with tritium concentrations of higher than 95% relative to all other hydrogenic isotopes. Higher tritium fractions cannot always be achieved, since a few percent (typically 2% to 4%) of hydrogen is needed for sufficient absorption of ion cyclotron waves due to the employed minority heating schemes. In addition, a very small minority of other hydrogenic isotopes is always present due to undesired legacy released from the wall, so that 95% tritium purity is considered as an arbitrary but useful lower limit within the given constraints, and we consider the relevant dynamics in the plasma at these purities to be dominated by tritium.

The H–T mixed plasmas presented here were investigated during the necessary transition from the campaign focussing on hydrogen plasmas to the campaign for tritium plasmas. At this early stage of the JET T-campaign, no neutral beam heating (NBI) systems were available, so that L–H transition studies could only be done with ion cyclotron resonance heated (ICRH) pulses. The use of ICRH had the additional advantage of lower tritium consumption compared to NBI heated plasmas being relevant to comply with the daily allowed tritium inventory limit, and ICRH enables smoother and more reliable heating power ramps, which increases the accuracy of the determination of P_{LH}. Due to the limitation in available heating power under these conditions, and in order to compare the tritium results with former results in deuterium and hydrogen plasmas, all experiments were performed with a magnetic field on axis of $B = 1.8$ T and a plasma current of $I_p = 1.7$ MA. One additional pulse from a later phase of the tritium campaign, which was heated with neutral tritium beams (T-NBI), was added for comparison with the ICRH results. All pulses had the same shape (called HT as described in reference [14]) with the outer divertor strikeline on the horizontal target, while the inner strike point was placed on the inner vertical target. The ion ∇B-drift was pointing towards the active X-point (lower single null).

The main result of our investigation is the good agreement of the measured L–H power threshold, P_{LH}, with the ITPA scaling (equation (1)) when isotope effects (i.e. the dependence according to equation (2)) and a reduction due to the metallic wall are taken into account *and* the radiated power is substracted. In order to demonstrate this, we first present the experimental strategy and time traces of some selected L–H transitions in order to discuss the dynamics of L–H transitions in ICRF heated, neutral beam heated and Ohmically heated plasmas of H–T mixtures and pure tritium (section 2). Section 3 deals with the power thresholds, P_{LH}, which were determined in the different tritium containing plasmas, and relates it to older data of P_{LH} in H and D with ILW. This section contains the main result of this study. In section 4, the role of radiation and the ion heating fraction are discussed, and conclusions are drawn in section 6.

2. Experimental strategy and dynamics of L–H transition pulses

The dedicated pulses to study the L–H power threshold in JET plasmas with ILW and finite tritium content were aiming at an accurate determination of the power threshold, P_{LH}, at different densities. For this purpose, slow ICRH power ramps (up to two per pulse) in the order of 1 MW s^{-1} at a constant density were performed. In order to maximize the absorbed power in ion-cyclotron radio frequency (ICRF) heated plasmas, the following heating schemes were used: for hydrogen–tritium mixtures, second harmonic heating ($\omega = 2\omega_{c,H}$) at hydrogen was applied. For pure tritium plasmas, hydrogen minority heating at the fundamental frequency ($\omega = \omega_{c,H}$) was used. One pulse heated with T-NBI was done for comparison in order to evaluate whether the results depend on the heating method.

On a pulse to pulse basis, the density was changed while keeping the power ramp the same. Since the available heating power of the ICRF system at JET was limited to 6 MW at the time of the tritium experiments, most of the L–H transition experiments were done at a comparably low magnetic field of $B = 1.8$ T, and only one pulse at $B = 2.4$ T. Otherwise the available heating power would not be sufficient to reach the L–H transition in the desired density range, especially in plasmas with high hydrogen concentrations due to the magnetic field and isotope dependence of P_{LH}.

For this study, we define the H-mode as a state of improved particle and energy confinement with respect to a given L-mode state as visible in a rise of density and temperature time traces at the edge, and a drop of edge transport for otherwise constant conditions. Consequently, the L–H transition time, t_{LH}, was determined as the time point at which the density started to rise and simultaneously the Balmer alpha line radiation, H_α, (or T_α in the T pulses) in the divertor dropped. At the same time the slopes of the edge temperature as well as the energy content of the plasma, W_{MHD} rose, too, and in most of the cases an M-mode [27] (also called I-phase [28]) appeared in the very same moment. The latter makes it difficult to identify the drop of the H_α signal, since the M-mode bursts can blur the signal in the time range, where the L–H transition happens. On the other hand, the signatures of the M-mode, which is considered to be part of the H-mode [27, 29], can easily be identified in magnetic probe signals, and therefore help to find H-mode phases. An L–H transition is only counted as a valid data point, if the H-mode phase sustained a few confinement times, i.e. approximately half a second or more. Otherwise we labelled it as *transient*, or if the H-mode transient phases appear repetitively (see below), as *dithering*.

We determined the L–H transition power threshold, P_{LH}, in two different ways. For comparison to existing multimachine scalings, we used $P_{LH} = P_{loss}(t_{LH})$, i.e. the loss power

$$P_{loss} = P_{Ohm} + P_{aux} - \frac{dW}{dt} \quad (4)$$

with Ohmic power P_{Ohm}, auxiliary heating power P_{aux} and the temporal change of the energy content of the plasma $\frac{dW}{dt}$. All quantities are averaged over 70 ms prior to t_{LH}. Due to the typically strong rise of the (diamagnetic) energy content W at the time point of the L–H transition, we do not take $\frac{dW}{dt}$ at t_{LH}, but 100 ms earlier than t_{LH} in order that P_{loss} is not affected by the L–H transition induced changes.

The other estimation of P_{LH} used is the power reaching the separatrix by transport in the plasma,

$$P_{sep} = P_{loss} - P_{rad} \quad (5)$$

with the radiated power of the bulk plasma P_{rad}. P_{sep} is considered to be more relevant than P_{loss}, since P_{rad} is most likely related to the core impurity content, which is considered to be irrelevant to the transition mechanism beyond the fact that it reduces the power available to heat the main plasma. $P_{LH} = P_{sep}(t_{LH})$ is therefore preferred to relate the results in tritium pulses to older findings in H and D plasmas. Otherwise,

the data is difficult to be compared due to the strong scatter of P_{loss} and the large contribution of P_{rad} to the total power balance in the plasma.

Due to a hardware fault in one of the ICRF generators, the phasing of the ICRF antennas was far from a perfect dipole (as desired) in several of the reported pulses. This had an impact on the RF wave absorption in the plasma and, thus, on the determined value of the L–H power threshold. When the antenna excites a substantial fraction of low $k_\parallel$ wave modes due to improper phase control, the so called RF heating efficiency is reduced compared to high $k_\parallel$ excitation as it is the case e.g. in perfect dipole operation. Therefore, the effective power absorbed in the plasma core is lower than the coupled power computed with the RF antenna signals only [23]. To take this effect into account, the actual toroidal spectrum excited by the antennas with the real-time phase measurements was computed for each pulse, and this was convoluted with the double-pass absorption computed with the 1D ICRF wave code TOMCAT [24]. This is done for each excited toroidal mode taking into account the main pulse parameters (density, temperature, magnetic field, etc). The calculations showed that a typical power correction of maximum 20% should be applied to the coupled ICRH power in the pulses of interest, therefore lowering the L–H power threshold in the tritium pulses by approximately 200 to 600 kW. In a dedicated pulse designed to validate these corrections i.e. with a first power ramp with pure dipole phasing and a second one mimicking the dephasing observed in the experiments, it was shown that the power corrections are adequate. Therefore, this correction was applied to all the pulses for which the antenna phasing was incorrect.

The concentration of the different hydrogenic species, H, D and T, were continuously monitored with an optical Penning (or species-selective Penning) gauge in the JET subdivertor region as described in references [25, 26]. It measures the concentration of one hydrogenic species relative to the total concentration of all hydrogenic species. Since the concentration of non-hydrogenic species was below 1% in all reported pulses, we directly used the output of the optical Penning gauge to determine A_{eff} from this data according to equation (3) ignoring contributions from heavier impurities (typically Be and Ni).

2.1. L–H transitions in ICRF heated H–T plasmas

The first series of pulses was performed during the necessary transition from pure hydrogen plasmas to pure tritium plasmas allowing for studying L–H transitions in different H–T mixing ratios. All pulses with a tritium concentration of up to 73%, were heated with ICRH at a frequency of 51.4 MHz corresponding to the second harmonic ($\omega = 2\omega_{c,H}$) in hydrogen. Most of the power absorbed by the plasma is deposited off-axis at about half radius. For tritium concentrations above 80%, hydrogen minority heating at the fundamental frequency ($\omega = \omega_{c,H}$) was employed corresponding to a wave frequency of $f = 32.2$ MHz. The power deposition in this case was off-axis again.

Figure 1 shows three examples of L–H transitions at different tritium concentrations. For low tritium concentration of 5% (figures 1(*a*), (d) and (g)), the L–H transition is very similar to a transition in a pure hydrogen plasma. This means that the L–H transition happened in the very last phase of the ICRH power ramp (figure 1(*a*), black line) at a comparably high power of $P_{ICRF} = 4.66$ MW, indicated by the strong increase of the edge density $\bar{n}_{e,Edge}$ (blue line), core density $\bar{n}_{e,Core}$ (black line), and the magneto-hydrodynamic energy content, W_{MHD} (red line), estimated from the equilibrium reconstruction, as shown in figure 1(*d*). P_{ICRF} is the power coupled from the ICRF antennnas into the plasma. The H-mode phase starting at $t_{LH} = 18.85$ s lasted only for 680 ms until the ramp down of the ICRF power. The tritium concentration was constant throughout the H-phase at around 5% (figure 1(*g*), black line).

For a medium tritium concentration of 39% as shown in figures 1(*b*), (*e*) and (*h*), the L–H transition happens already at a substantially lower power of $P_{ICRF} = 3.56$ MW at 16.93 s. This indicates that a higher tritium concentration in the plasma leads to a lower P_{LH} in agreement with the expected mass scaling of $P_{LH} \propto 1/A_{eff}$. The large fluctuation of the coupled ICRF power and other quantities in the H-mode phase is caused by large type-I ELMs.

For the highest tritium concentrations of 98.5%, as shown in figures 1(*c*), (*f*) and (*i*), H-mode is achieved already at a power of $P_{ICRF} = 2.02$ MW. This is much lower than the necessary powers at the L–H transition for lower tritium concentrations, and supports the suggested isotope scaling of the L–H transition (equation (2)). At this high tritium concentration, ICRF minority heating at the fundamental frequency of hydrogen was applied.

A very prominent observation is the comparably high radiated power P_{rad} (figure 1(*c*), blue line) during the H-mode phase after the L–H transition, which seems to increase with higher tritium concentration. The radiated power signal was measured with the vertical bolometer camera [32], and is for the considered pulses in excellent agreement with the bulk plasma radiation inside the normalized poloidal flux radius of $\rho_{pol} < 0.95$ determined from 2D bolometric reconstruction taking into account all bolometer channels (including the horizontal camera) with a method described in reference [33]. This trend of higher radiated power in ICRF heated T-containing plasmas is a general observation we made in this study and will be discussed in more detail in section 4.

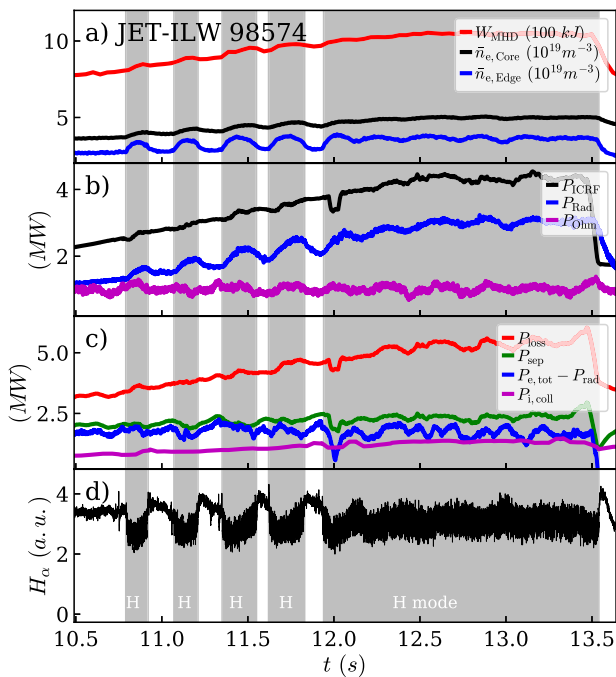### 2.2. L–H transitions in ICRF heated pure T plasmas

For tritium concentrations above 95%, we consider them as *pure* tritium plasmas since the behaviour and dynamics of these pulses is dominated by tritium. For this type of plasmas, hydrogen minority heating at the fundamental frequency ($\omega = \omega_{c,H}$) was used corresponding to an injected wave frequency of $f = 32.2$ MHz.

Several attempts to achieve a stationary H-mode in pure tritium plasmas at medium densities failed, and only dithering L–H transitions, i.e. a repetitive alternation between short L-mode and H-mode phases were observed. Only for comparably high densities, four stationary H-mode phases were
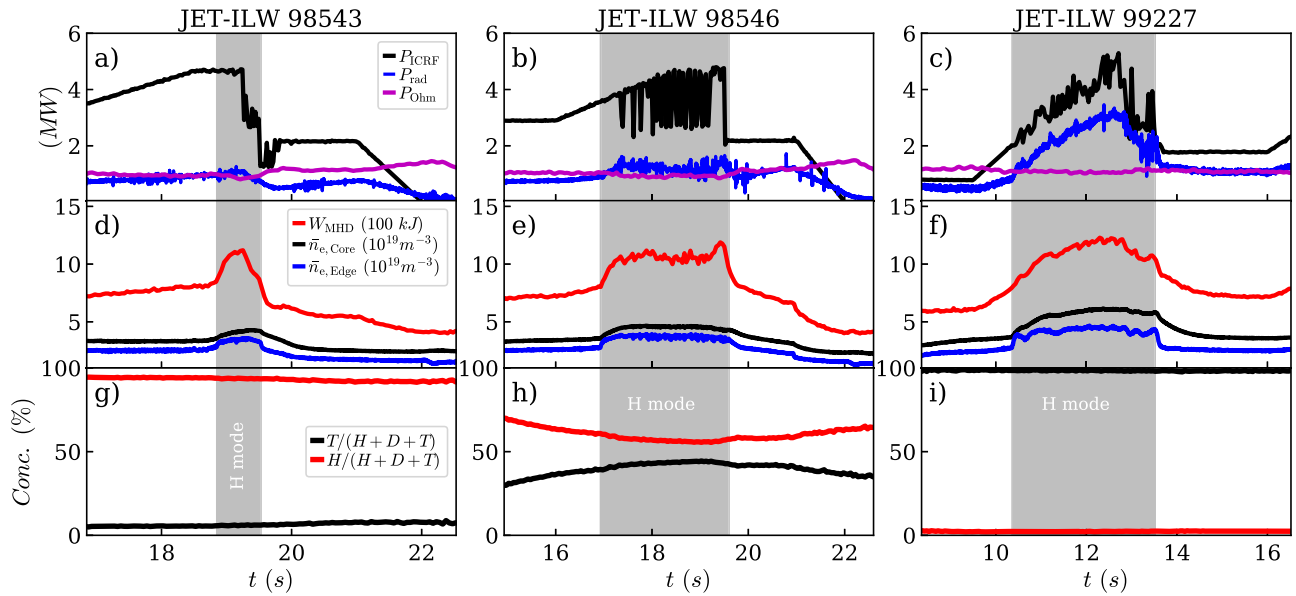
Figure 1. L–H transitions in ICRF heated plasmas with different T concentrations. (*a*) Low T-content (5%). (*b*) Medium T-content (39%). (*c*) High T-content (94%). The necessary power to access the H-mode (grey shaded area) decreases with increasing T-concentration. The radiated power systematically increases with the T-concentration in H-mode phases of ICRF heated plasmas.

Figure 2. L–H transitions in an ICRF heated pure T plasma. P_{sep} (green in panel (*c*)) increases step by step during the L–H dithering until the plasma enters a sustained H-mode at 11.94 s. Similarly, the heating power collisionally transferred to the ions, $P_{i,coll}$ (purple line in panel (*c*)), increases until the final H-mode is achieved. The net power to electrons (blue line in panel (*c*)), however, does not systematically rise during the dithering ramp.

achieved. Since two of them were with undesired ICRH antenna phasings, and two with the correct settings, we conclude that the antenna phasing is not decisive to get a stationary H-mode. For the highest density, a stationary H-mode was reached only after a series of a few L–H dithers. This pulse is shown in figure 2.

The dithering occurs very often during slow power ramps in the high density branch. The reason for dithering cycles is the following: during the heating ramp, the plasma enters the H-mode when the heating power, or more precisely P_{sep}, exceeds the (density dependent) power threshold $P_{LH}(n)$. Due to this, the confinement improves and, thus, the density rises. If the heating ramp is sufficiently slow, this rise in density, dn/dt, can let the plasma drop out of H-mode if

$$\frac{P_{sep}}{dt} < \frac{P_{LH}}{dn} \cdot \frac{dn}{dt}. \tag{6}$$

This means that the operational point of the plasma moves to the right in the P_{LH}-density plane (like figure 5) and falls back into L-mode again. This dropping out of H-mode is facilitated by two further contributions: first, the dW/dt term in P_{sep} is typically rising after the L–H transition, hence, lowering P_{sep}, and, second, the improved confinement typically leads to higher impurity concentration and, hence, higher radiation, P_{rad}, which likewise lowers P_{sep}. At some point, while the heating ramp continues, P_{sep} exceeds again P_{LH} and the L–H–L cycle can start from the beginning.

The described dithering dynamics is clearly visible in figure 2. Due to the rise of the ICRF power, P_{ICRF} (black line in (*b*)), likewise P_{loss} (red in figure 2(*c*)) and P_{sep} (green in figure 2(*c*)) increase. This leads to a first L–H transition at 10.79 s. The improved confinement at this point in time let the density increase (blue and black lines in figure 2(*a*)). At the same time, the radiation, P_{rad} (figure 2(*b*), blue line), increases due to the higher density, which in general increases the level of Bremsstrahlung and the line radiation. This lets P_{sep} drop in the first moment after the L–H transition. The dW/dt term does not play a significant role here, since the variation of plasma energy is small in this case. The lowered level of P_{sep} due to radiation and the rise in density, which increases P_{LH}, leads to

a back transition to L-mode at 10.92 s. In the following, the lower radiation during the L-phase lets P_{sep} recover quickly and, since the heating power ramp continues, P_{sep} is further boosted. Due to the falling density and the rising P_{sep} during the L-mode phase P_{sep} exceeds P_{LH} again at 11.07 s, and the second L–H transition occurs. This cycle repeats until a stationary H-mode phase is achieved at $t_{\text{LH}} = 11.94$ s due to a comparably large excursion of P_{sep} before.

As discussed, P_{sep} is rising step by step during the dithering until the stationary H-mode is achieved. Similarly as P_{sep}, the heating power collisionally transferred from the high energetic ICRH ions to the bulk ions, $P_{\text{i,coll}}$, estimated by means of PION simulations [46], rises continuously during the dithering (see purple line in figure 2(*c*)). As discussed in more detail in section 4.2, we assume that a higher edge ion heat flux is beneficial for the H-mode access. Due to the lack of ion temperature measurements, we cannot directly determine the edge ion heat flux, but use the heating power to the ions, $P_{\text{i,coll}}$, as a proxy for it. This approach has certainly limitations, since it does not take into account the collisional electron–ion energy transfer. But it is indicative, that the transition to the sustained H-mode correlates with the maximum of $P_{\text{i,coll}}$ during the evolution of the heating power ramp.

This is not the case for the net power to electrons, $P_{\text{e,tot}} - P_{\text{rad}}$ (blue line in figure 2(*c*)), which seems to saturate after the second dither and even exhibits a decreasing tendency. Here, the total power to electrons, $P_{\text{e,tot}}$, serves as a proxy for the edge electron heat flux and is the sum of three contributions: the direct heating of electrons by the ICRF wave and the collisionally transferred power to electrons from the heated ion species (minority H in this case) and the Ohmic power. The first two contributions were estimated with PION simulations. The similar behaviour of $P_{\text{i,coll}}$ and P_{sep} indicates that these two quantities are related to each other. It is suggested that they are crucial for the triggering of the L–H transition, since the stationary H-mode is achieved only when they have reached their maximum values. If $P_{\text{i,coll}}$ is interpreted as a proxy for the edge ion heat flux (a higher relative ion heating will favour a higher edge ion heat flux), this result supports the idea of a critical edge ion heat flux as raised by Ryter *et al* [21].

One attempt to achieve an H-mode in an ICRH T-plasma was likewise undertaken in a plasma with a magnetic field of $B = 2.4$ T and a plasma current of $I_{\text{p}} = 2.0$ MA. Similar to most of the pulses with ICRF heating at $B = 1.8$ T, the pulse at 2.4 T exhibited only a dithering, but no sustained H-mode.

Overall, a few sustained H-mode phases were achieved in ICRF heated pure tritium plasmas at comparably high densities with the available heating power of up to 6 MW. Apart from this sustained H-modes, many dithering L–H transitions with short transient H-mode phases were observed, so that it can be concluded that access to sustained H-modes with ICRH in JET-ILW can be more difficult to be achieved in pure tritium plasmas than in H–T mixtures or pure H or pure D plasmas. This result is probably related to the comparably high radiation levels in these pulses, which might be related to the fact that the presence of tritium can increase the sputtering on plasma facing components in ICRF heated plasmas (see discussion in section 4). The undesired antenna phasing of the ICRH does
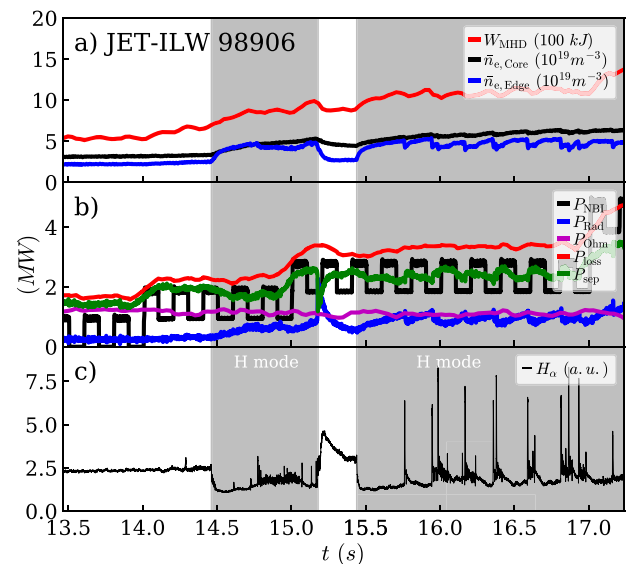
Figure 3. L–H transitions in T-NBI heated pure T plasmas. The first H-mode phase during the NBI power ramp starts at 14.46 s and is terminated after an impurity event, which let P_{sep} drop due to the increase in radiation. After the recovery of P_{sep}, a long and sustained H-mode phase with large edge localized modes follows.

not seem to be causal for the higher probability of dithering transitions, since also pulses with proper antenna phase control exhibited dithering transitions.

2.3. L–H transitions in T-NBI heated plasmas

For L–H transition studies, more experimental time was devoted to ICRF heated tritium plasmas than to T-NBI heated plasmas, since the ICRH system was available earlier during the tritium campaign and the tritium consumption is much less in ICRH plasmas compared to plasmas heated with T-NBI allowing for more pulses within the given daily tritium inventory limit of the machine. Nevertheless, one pulse with T-NBI was dedicated for the comparison with ICRF heated pulses at 1.8 T. Parts of this pulse are shown in figure 3.

All NBI sources in these experiments where injecting pure neutral tritium beams with about one MW per source. For a comparably smooth heating power ramp, one T-NBI source was modulated with a duty cycle of 50% (100 ms beam on), and then consecutively additional sources were added. The first T-NBI induced L–H transition appears at 14.46 s when P_{loss} reaches 2.24 MW. P_{sep} is slightly lower at 1.96 MW (see figure 3(*b*)). The following H–L transition happens due to a sudden increase of P_{rad}, which let P_{sep} drop significantly. The peak in radiation is related to influx of tungsten, which appeared after a few very large type-I edge localised modes (ELMs).

After a short L-mode phase of about 260 ms, the radiation drops and P_{sep} recovers, so that the next L–H transition takes place at 15.44 s. The required P_{sep} is higher in this case than before, which is related to the increased density since the last L–H transition. The following H-mode phase contains large type-I ELMs, but no major impurity influxes appeared. The H-mode is sustained for the remainder of the pulse.

2.4. L–H transitions in Ohmically heated plasmas

Before and after the ICRH or NBI heated phases, which were devoted to study the H-mode power threshold during power ramps, a few unintended L–H transitions occurred in purely Ohmic phases at low density. This is a peculiar feature of tritium containing plasmas at JET due to their (expected) low power threshold, since Ohmic L–H transitions were not observed in D, H or He plasmas at 1.8 T (apart from an exception in D, which could not be reproduced). As in ASDEX Upgrade [34], the Ohmic transitions were only observed at low densities. In contrast to observations at other fusion devices [35–37], we did not find Ohmic L–H transitions at higher densities in our experiments.

All the Ohmic H-mode phases feature a strong M-mode activity, and, probably due to a low neutral gas inventory at these low densities, only a comparably small rise in density. The rise of the plasma energy content, the edge temperature (not shown) and the drop of the T_α signal, however, unambiguously demonstrate the confinement improvement.

Three different types of Ohmic H-mode phases were found:

(a) Short Ohmic H-modes during the density build-up at low density. These H-modes were terminated by a rise or a drop in density. An example is shown in figures 4(*a*), (*d*) and (*g*). In this case the drop of the H_α signal is blurred by the appearance of the M-mode bursts. The L–H and H–L transitions happen at similar values of density and P_{sep}. The radiation is very low and constant. The dynamics of this pulse indicates that there is a low density branch of P_{LH}, and the H-mode is approached from (and left towards) the low density side.

(b) Short Ohmic H-modes starting a few 100 ms before or at the very beginning of the ICRH power ramp. This phase is terminated during the ICRH power ramp possibly due to the increased radiation, when the ICRH was switched on. An example is shown in figures 4(*b*), (*e*) and (*h*). During this pulse the ICRH antenna polarity was not a usual dipole (relative phase at some of the antenna straps of 120 degree instead of 180 degree), which can lead to a lower wave absorption and higher radiation levels induced by increased plasma wall interaction. Despite the apparent increase of P_{sep} the pulse drops out of H-mode at 14.3 s. This indicates that unfavourable antenna settings can prevent the pulse from staying in H-mode.

(c) Ohmic H-modes at the very end of the pulse, when the ICRH power was switched off and the radiation went down. These H-mode phases continued during large parts of the current and magnetic field ramp down phase of the pulse. An example for this is shown in figures 4(*c*), (*f*) and (*i*). The L–H transition is reached when P_{sep} has stabilized after its decrease. A very slight increase in density, a drop of the radiation and a jump of the outer wall gap (distance between LCFS at the midplane and the outer wall) temporally correlate with the L–H transition. Thus, it is difficult to conclude which parameter is decisive. However, the fact that the radiation possibly plays a role for

the Ohmic transitions of type (b) as discussed before, it might be the case that the high levels of P_{rad} prevented an earlier L–H transition also in this case.

3. The L–H power threshold in tritium containing plasmas

The experimentally determined L–H power thresholds, P_{LH}, of the tritium containing plasmas presented in section 2 given in terms of P_{loss} are shown in figure 5, left, and estimated from $P_{sep} = P_{loss} - P_{rad}$ are shown in figure 5, right. The abscissa of these figures is the line averaged electron density, $\bar{n}_e$, measured with a central vertical interferometer chord. The asymmetric error of P_{loss} and P_{sep} given as vertical lines, was determined by the maximum value (upper bound) and the minimum value (lower bound) of P_{loss} and P_{sep}, respectively, which occurred in the time interval 200 ms prior to the L–H transition. This way it takes excursions and variations of the signals into account, which appear in the order of one energy confinement time τ_E prior to the L–H transition.

The ICRH pulses in H–T mixtures are shown as open red diamonds with the tritium concentration of the plasma given in percent. These plasmas were heated with ICRF 2nd harmonic heating of hydrogen. For the lowest T-concentration of 5%, the power threshold of about 6 MW is in the range of pure hydrogen plasmas indicated with red circles corresponding to data from pure ICRF heated hydrogen plasmas in older campaigns in JET-ILW partially published in reference [14]. With increasing T-concentration (27% and 39%), the power threshold decreases monotonically by more than 1 MW. This is in line with the expected isotope mass scaling, which predicts a lower power threshold for a higher tritium concentration.

At higher tritium concentrations above 90%, the ICRF heating scheme was changed to hydrogen minority heating at the fundamental frequency. For these plasmas four transitions in a density range from 3.5 to 4.46 $\times$ 10^{19} m^{-3} were found (magenta filled diamonds). The data point at highest density corresponds to the L–H transition into the longest H-mode phase shown in figure 2. P_{loss} at this L–H transition is on the same level as the P_{loss} of the plasma with 39% T-concentration. P_{sep}, however, is significantly lower and is even lower than P_{LH} of ICRF heated deuterium plasmas (blue squares) at highest densities, which were investigated in former campaigns with ILW [14].

As mentioned in section 2, most of the pulses in pure tritium plasmas exhibited L–H dithering. For these transient H-mode phases, P_{LH} was analysed in the same way as the other L–H transitions and the respective L–H transition powers are shown as magenta crosses in figure 5. The shown data points during the dithering and other transient phases without repetitions (both labelled as 'transient') have larger error bars, because the plasma parameters prior to these transitions are varying significantly. Nevertheless, the data points from dithering phases line up very well in the P_{sep}-density plane (figure 5, right). They are on the same level or sometimes lower than P_{sep} in
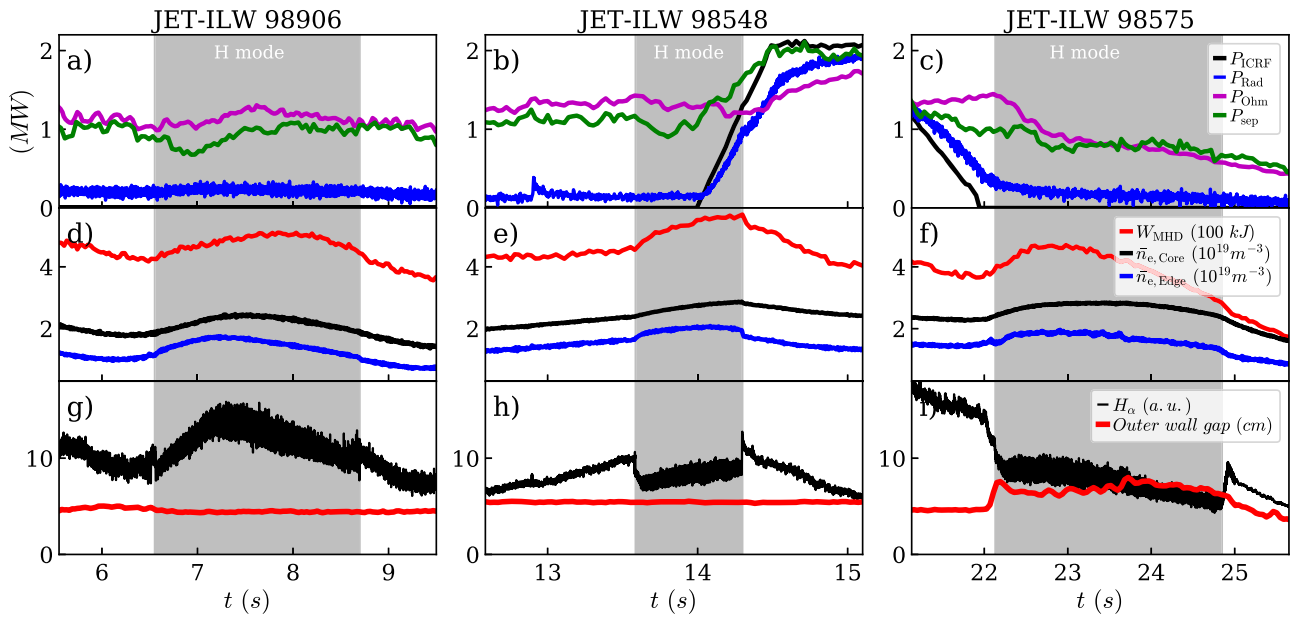
Figure 4. L–H transitions in Ohmically heated phases in pure tritium plasmas. Either the Ohmic H-phases are terminated by a drop in density (*a*), (*d*) and (*g*) or after the ICRH with unfavourable antenna settings has been switched on (*b*), (*e*) and (*h*). Ohmic H-phases, which appear at the very end of some pulses (*c*), (*f*) and (*i*), occur after the ICRH is switched off and start temporally correlated with a drop in radiation and during a jump of the gap between plasma and the outer wall at the outer midplane.
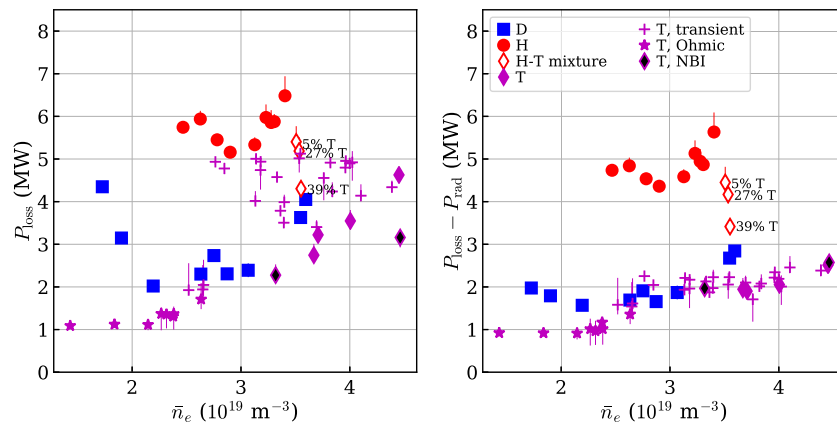
Figure 5. The L–H power threshold in T plasmas (magenta symbols) determined in terms of P_{loss} (left) and P_{sep} (right) against line-averaged density $\bar{n}_e$. P_{LH} data of ICRF heated plasmas in D (blue squares) and H (red circles) are shown for comparison. The H–T mixed plasmas are shown as open red diamonds. All symbols correspond to ICRF heated plasmas except for the Ohmic T plasmas (stars) and T-NBI pure T pulses (black coloured diamonds). Only four sustained H-modes (magenta filled diamonds) were found in ICRF heated pure T plasmas. The other data of ICRF heated pure T plasmas were determined in dithering or other transient phases (magenta crosses).

comparable deuterium plasmas. This confirms the overall trend of ICRF heated tritium plasmas, that the power threshold is equal or slightly lower than deuterium plasmas and, therefore, qualitatively agrees with the expected isotope mass scaling of P_{LH}. This is, however, only true for P_{sep} (figure 5, right). P_{loss} (figure 5, left), on the other hand, is typically higher in transient ICRF heated pure tritium plasmas than in deuterium due to high radiation levels. The fact that P_{loss} of several ICRF heated pure tritium plasmas led only to dithering transitions, although the injected power was almost on the same level as sustained H-modes in hydrogen, is surprising and obviously related to high radiation levels.

The L–H transitions observed in Ohmically heated phases of tritium containing plasmas are marked as magenta stars in figure 5. All Ohmic L–H transitions group at very low densities and appear at power levels in the range of 1 MW, which is about a factor of two lower than for comparable deuterium pulses and about a factor of 4 to 5 lower than for the lowest P_{LH} in hydrogen pulses, which were restricted to higher densities. This low value of P_{LH} in Ohmic pulses is qualitatively in agreement with the expected isotope mass scaling of P_{LH}.

The single tritium pulse, which was heated with T-NBI, had two L–H transitions at different densities (black diamonds in figure 5). These T-NBI data points are on the same level as the ICRH data points for tritium plasmas in terms of P_{sep} (right),

but much lower in terms of P_{loss} due to the fact that the radiated power P_{rad} is much lower in T-NBI heated plasmas compared to ICRH plasmas.

The power thresholds, P_{sep}, of the Ohmic, ICRF heated, T-NBI and the transient transitions in tritium plasmas line up quite well and cover the full density range from 1 to 5×10^{19} m^{-3}, which is a larger accessible density range than achieved for deuterium or hydrogen plasmas. The values of P_{sep} are systematically rising above 2.5×10^{19} m^{-3}, which can be considered as the high density branch. A clear low density branch as visible for D and H is not observed for pure tritium plasmas. Either there is no clear minimum for tritium plasmas, or $\bar{n}_{e, min}$ and the low density branch is at densities lower than the lowest Ohmic tritium data point. However, as it is shown in figure 4(*a*), the pulse enters H-mode during a rise in density and exits the H-mode phase during a drop of density while P_{sep} is quite constant. This dynamics indicates that the Ohmic transitions are close to or at the low density branch.

The P_{LH} data shown in figure 5 is presented again in a different manner in figure 6 in order to illustrate better the effective isotope mass dependence of P_{LH}: the abscissa here is the ITPA scaling [2] extended by the suggested isotope scaling $P_{LH} \propto A_{eff}^{-1}$ [10]. We refer to this scaling

$$P_{scal,iso} = 0.049\bar{n}^{0.72}B_t^{0.8}S^{0.94}2 \cdot A_{eff}^{-1} \qquad (7)$$

as the isotope dependent ITPA scaling (isoITPA). Since the original ITPA scaling was done for deuterium plasmas with effective isotope mass of $A_{eff} = 2$, equation (1) is extended by a factor of $2 \cdot A_{eff}^{-1}$ to get equation (7). This scaling serves as our reference for the following discussion.

A black dashed line in figure 6 indicates the isotope dependent ITPA scaling equation (7), however, reduced by 20% in order to take into account the well documented fact [3, 31], that P_{LH} is at least 20% lower in a metallic wall compared to the original ITPA scaling, which was derived from carbon wall data. More specifically, the full formula of the suggested scaling corresponding to the black dashed line in figure 6 reads

$$P_{scal,ILW} = 0.049\bar{n}^{0.72}B_t^{0.8}S^{0.94} \cdot 2 \cdot A_{eff}^{-1} \cdot 0.8. \qquad (8)$$

Expressed in terms of P_{loss} (figure 6, left), the hydrogen data (red circles), the majority of the deuterium data (blue squares), the Ohmic tritium pulses (magenta stars) and the T-NBI heated tritium pulses (black diamonds) agree very well with the modified scaling $P_{scal,ILW}$ (equation (8), black dashed line). However, the majority of the ICRF heated tritium pulses in pure tritium (magenta crosses and solid diamonds) and in H–T mixtures (red open diamonds) are up to a factor of 2.5 above the modified scaling $P_{scal,ILW}$. This confirms the observation presented above, that the ICRF heated tritium containing plasmas and pure tritium plasmas violate the expected mass scaling of P_{LH}.

For P_{sep} (figure 6, right), we get a modified picture: the Ohmically heated tritium data, and the (ICRF heated) deuterium and hydrogen data align quite well below $P_{scal,ILW}$ (black dashed line), and are close to the grey line, which indicates the isotope dependent ITPA scaling reduced by 40%. Due to the facts, that the subtraction of P_{rad} lowers P_{sep} with respect

to P_{loss} and that the ITPA scaling was derived from P_{loss} data, it is natural that the experimental data points of P_{sep} are below the scaling line of $P_{scal,ILW}$. This is in agreement with the result presented in reference [31] that P_{sep} in JET-ILW is about 40% lower than the (unmodified) ITPA scaling (equation (1)). The T-NBI data as well as the data of ICRF heated pure tritium and mixed plasmas are very close to the scaling line acc. to equation (1), i.e. do not exhibit the 40% reduction with respect to the isotope dependent ITPA scaling, but only the 20% reduction. The scatter of tritium data in terms of P_{sep} is lower than in the P_{loss} data. The reason for this are large values of P_{rad} in some of the experimental data points leading to high values of P_{loss}, which appear corrected for this effect in the P_{sep} graph.

Overall, the power thresholds in terms of P_{sep} in Ohmic L–H transitions of pure tritium plasmas line up very well with the data of deuterium and hydrogen plasmas in metallic wall conditions indicating a 40% reduction with respect to the isotope dependent ITPA scaling. However, pure tritium plasmas and H–T mixed plasmas heated with ICRF or T-NBI are clearly above this line, and tend to be better described by $P_{scal,ILW}$. This indicates that the $1/A_{eff}$-dependence of the power threshold is not fulfiled for these plasmas.

4. Impact of radiation and heating scheme on P_{LH}

As described in the previous sections, a prominent observation of our investigation is the unexpectedly high power threshold in terms of P_{loss} of ICRF heated plasmas with tritium concentrations of 27% or more, and the slightly higher P_{sep} of ICRF and T-NBI heated plasmas compared to Ohmic tritium, deuterium and hydrogen plasmas. But what is different in these plasmas compared to the older deuterium and hydrogen plasmas?

4.1. Influence of radiation

The first parameter, which might explain the higher P_{loss} in ICRF heated tritium plasmas, could be the radiated power, P_{rad}. This quantity, determined at the time point of the L–H transition, is shown in figure 7 in the same representation as the P_{LH} graphs before.

The radiated power, P_{rad}, is higher in ICRF heated pure tritium plasmas than in ICRF heated deuterium or hydrogen plasmas. The highest values of P_{rad} are achieved for transient (more specifically dithering) transitions. Lowest levels of P_{rad} are, however, observed in T-NBI heated and Ohmic tritium plasmas. The H–T mixed plasmas have intermediate radiation levels comparable to the hydrogen plasmas. Thus, the high levels of radiation in ICRF heated pure tritium plasmas seem to be intrinsically related to the heating scheme, and not (only) to the fact that tritium is the main isotope.

The properties of the radiated power in tritium plasmas is currently under investigation during the ongoing campaign in JET. First studies [38] in helium plasmas confirm that helium plasmas are more effective in sputtering of Be and W due to the higher isotope mass compared to hydrogen or deuterium
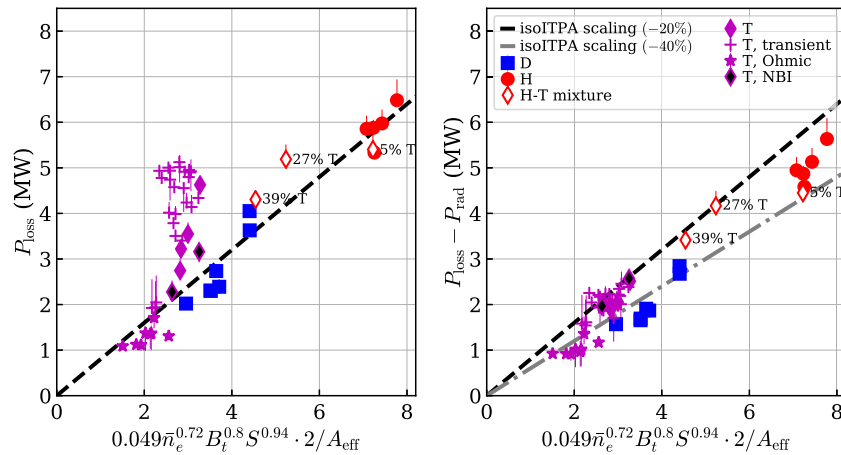
Figure 6. L–H data in terms of P_{loss} (left) and P_{sep} (right) vs the isotope dependent ITPA scaling (equation (7)). The data are the same as in figure 5. The black (grey) dashed line corresponds to the isotope dependent ITPA scaling reduced by 20% (40%) in order to take the effect of a metallic wall into account corresponding to equation (8). The Ohmic and T-NBI heated T data is in very good agreement with the scaling, but the ICRF heated pure tritium and, to a minor extend, the H–T mixed plasmas have significantly higher power thresholds (left). When the radiation is subtracted (right), most of the data points from D, H and Ohmic T plasmas align with the isotope dependent ITPA scaling reduced by 40%, while the T-NBI, and the ICRF heated tritium data are around the scaling line indicating the isotope dependent ITPA scaling reduced by 20%.
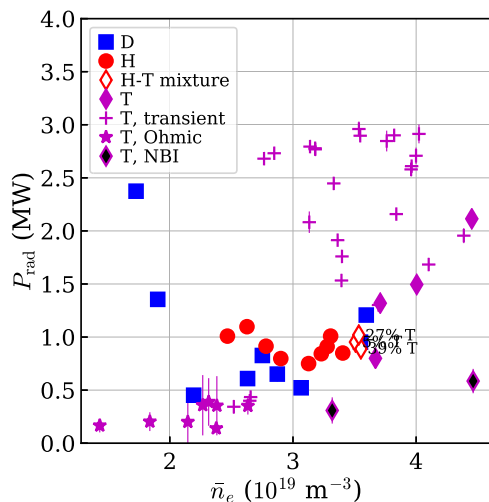
Figure 7. Radiated power at the L–H transition in different plasmas in the same representation as the power threshold data in figure 5. Ohmic T and T-NBI heated plasmas have lowest radiation levels, while ICRF heated pure tritium dithering plasmas show the highest levels of radiation. The ICRF heated D and H shows moderate to low radiation levels.

plasmas, and the relatively higher Be content in the scrape-off layer of helium plasmas synergistically increases the sputtering of Be on W further. Therefore, helium plasmas contain more impurities and radiate more. The same effect of increased sputtering (see also reference [39]) due to the higher isotope mass and, hence, a higher level of radiation due to impurities is likewise expected in tritium plasmas. This is particularly the case for ICRH plasmas, which tend to higher radiation levels due to sputtering by means of strong rectified parallel electric field components in the scrape-off layer [40]. This could explain the high radiation levels in ICRF heated pure tritium plasmas. In addition to this possible enhanced sputtering of

tritium in combination with ICRH, the unfavourable antenna spectrum due to undesired phasing in some of the pulses have certainly increased the tendency to higher radiation levels. Pulses with unfavorable antenna phasing had systematically higher radiation fractions ($P_{\mathrm{rad}}/P_{\mathrm{loss}} > 40\%$) than pulses with proper antenna phasing ($P_{\mathrm{rad}}/P_{\mathrm{loss}} \approx 20\%$).

This behaviour was confirmed in a dedicated plasma with proper antenna phasing ($180°$ corresponding to a dipole) in the first power ramp and an unfavourable antenna phasing ($130°$) in the second power ramp. The radiation at the L–H transition in the first and second ramp occurred at the same line-averaged density and the radiated power was 0.8 MW for the proper antenna phasing compared to 1.3 MW for the unfavourable antenna phasing. This seems to be a clear effect of the unfavorable antenna phasing. However, it cannot be excluded that impurities accumulate during the plasma pulse duration independent of any ICRH effect, and in dithering transitions we clearly found that the radiation was higher when the L–H transition took place in a later phase of the plasma [41].

In general, the relatively low heat and particle transport in tritium plasmas compared to hydrogen or deuterium plasmas further increases the ability of the plasma to confine impurities leading to elevated radiation levels, which were very prominently rising in H-mode phases of plasmas with consecutively increased tritium concentration (see figure 1).

Although we saw clearly that the radiation is higher in ICRF heated pure tritium plasmas than in Ohmic, T-NBI heated, ICRF heated D or H plasmas, P_{rad} alone cannot explain why ICRF heated tritium containing and pure tritium plasmas show a slightly higher power threshold in terms of P_{sep} compared to the other types of plasmas. Even after subtraction of P_{rad}, the small deviation of ICRF heated tritium containing plasmas and pure tritium plasmas from the mass scaling was still visible in P_{sep}, especially for H–T mixtures. Likewise the T-NBI heated plasma exhibited higher relative power thresholds than

expected from the metallic wall scaling. Thus, additional physical processes beyond radiation might play a role for the higher P_{LH} of ICRF and T-NBI heated tritium containing and pure tritium plasmas.

4.2. Heating power distribution

The distribution of heating power in the plasma, especially the heating power contributions, which are deposited to the thermal ions or electrons, can have a strong impact on P_{LH}. Very detailed studies in ASDEX Upgrade (AUG), which has a high flexibility to change from dominant electron to dominant ion heating by an appropriately chosen heating mix of electron-cyclotron resonance and NBI, revealed that the ion heat flux at the edge is a key quantity determining P_{LH} in plasmas with low torque [21]. This was confirmed in Alcator C-mod, and according to the findings, the L–H transition occurs, when the edge ion heat flux exceeds a certain critical value, which depends on density, magnetic field, the plasma surface [30] and on the plasma isotope [11]. This concept of a critical edge ion heat flux is possibly related to an underlying critical perpendicular flow velocity at the very edge [31, 42] and can explain the appearance of the low density branch of P_{LH} by the effect of a lacking electron–ion energy transfer in predominantly electron heated plasmas at low densities [21, 43]. It is not clear yet whether the concept of a critical ion heat flux at the L–H transition also applies to JET plasmas, since the effect of NBI-induced torque [44] complicates the picture, and there are indications that a critical $E \times B$ velocity, which can be considered as the underlying reason for the critical ion heat flux [31, 42, 43], could not be confirmed in all types of plasmas [45]. Nevertheless, we assume for the following discussion, that a higher edge ion heat flux is beneficial for the H-mode access.

Due to the lack of ion temperature measurements in all considered pulses it was not possible to determine the edge ion heat flux directly from a proper transport analysis of the experimental kinetic profiles. However, we estimated the collisionally transferred power to bulk ions or electrons by the respective heating schemes by means of the PION code for the ICRF heated pulses [46] and PENCIL [47] for the T-NBI heated pulses. This approach neglects the redistribution of power by transport processes and collisional effects. Most prominently the electron–ion heat transfer between thermal bulk ions and electrons is not taken into account. Nevertheless, the initial power distribution due to the respective heating scheme can serve as a proxy for the edge ion heat flux, since e.g. a dominantly ion heated plasma typically exhibits a higher edge ion heat flux than a dominantly electron heated plasma.

The results of the PION modelling (including the correction factors due to the partially wrong antenna phasing) and PENCIL simulations at the time points of the L–H transition are shown in figure 8. The left panel (*a*) shows the volume integrated power transferred to bulk *ions*, $P_{i,coll}$, from fast resonant ions, i.e. the power originating from the heating species (suprathermal ions from ICRH or NBI) after collisional transfer. The highest power levels arrive at the ions for hydrogen plasmas (red circles). Deuterium (blue squares) and tritium

plasmas (magenta crosses and diamonds) have similar power levels, with a tendency that tritium plasmas, particularly T-NBI tritium plasmas, have a lower power to ion level than deuterium plasmas. The power levels to ions very clearly decrease monotonically with increasing tritium concentration in H–T mixed plasmas (red open diamonds). Qualitatively, the data points in H, D, H–T mixed and T plasmas indicate that a higher effective isotope mass correlates with a lower (necessary) power level into the ions. If the power level to ions is understood as a proxy for the edge ion heat flux $Q_{i,edge}$, the data suggests, that $P_{i,coll}$ depends, like P_{LH}, inversely on the effective isotope mass as discussed in reference [43], i.e.

$$Q_{i,edge} = 0.0029 \bar{n}^{1.05} B_t^{0.68} S^{0.93} A_{eff}^{-1} \quad (9)$$

with the $Q_{i,edge}$ in MW, line-averaged core density $\bar{n}$ in units of 10^{20} m^{-3}, toroidal magnetic field B_t in T, surface area S of the LCFS in m^2 and effective isotope mass A_{eff}.

The observed trend of the isotope mass dependence confirms the finding in AUG plasmas [11], where a higher edge ion heat flux was needed in hydrogen compared to deuterium for accessing the H-mode, although the difference in our data (about a factor of 4 between hydrogen and deuterium) is higher than reported from AUG (factor 2). It is remarkable, that figure 8(*a*), displaying the power to ions, $P_{i,coll}$, looks qualitatively similar to figure 5, right, which shows P_{sep}: low values for D and T, but high values for H. Overall, the power threshold, P_{sep}, and the power to ions, $P_{i,coll}$ (considered as a proxy for the edge ion heat flux), seem to be linked to each other.

The isotope dependence of the power, which is collisionally transferred from the heating species to the *electrons* (including direct wave heating of electrons), $P_{e,coll}$, is shown in figure 8(*b*). The ICRF heated H–T mixed plasmas and transient pure tritium plasmas exhibit the highest levels of power to the electrons. The medium density ICRF heated pure tritium plasmas have comparably low electron heating contributions. The deuterium and hydrogen data is quite scattered but, in general, the power to electrons in deuterium and hydrogen plasmas tends to be lower than in tritium containing plasmas and transient pure tritium plasmas.

The ratio of the power to ions to the total power at the L–H transition, $P_{i,coll}/P_{tot}$ (see figure 8(*c*)), features a quite clear isotope dependence. Hydrogen has the highest share of ion heating (around 60%) while deuterium is lower (around 40% at medium density). Tritium plasmas, especially T-NBI heated and transient ICRF heated L–H transition data points, exhibit the lowest share of ion heating. This is most probably related to the heating schemes. The ICRF heated pure tritium data was obtained in plasmas heated at the fundamental of hydrogen in a minority of hydrogen ions in pure tritium plasmas. For these schemes, the power of the incoming ICRF wave is transferred to a minority of plasma ions while the tritium concentration is high, i.e. more *power per ion* is absorbed at the directly heated (fast) ion population than in the case of comparable majority heating schemes. Therefore, the wave heated minority ions have higher energies, and, thus, preferentially heat the bulk electrons by collisions. In contrast to this, the ICRF majority
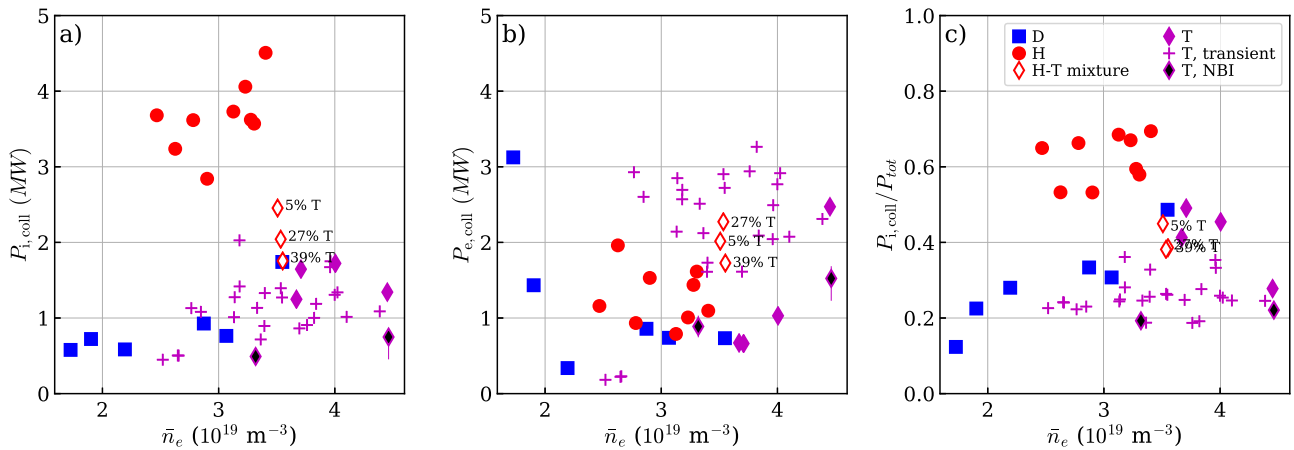
Figure 8. Power transferred from the heating species to ions (*a*) and to electrons (*b*) by collisions as estimated with PION for the ICRH data and PENCIL for the T-NBI data at the time point of the L–H transitions. The power to electrons in (*b*) contains additionally the direct wave heating of electrons. (*c*) Relative heating power to ions normalized to the total heating power (including Ohmic heating). Symbols are the same as in figure 5.

heating schemes as employed in hydrogen plasmas predominantly heat the ions, since the ICRH wave energy is coupled to a larger number of ions, so that they are less energetic and, thus, favouring ion heating.

Interestingly, the ICRF heated pure tritium plasmas at medium density (magenta diamonds) exhibit much higher shares of ion heating compared to the transient ICRF heated pure tritium L–H transitions (crosses). This supports the idea that a higher ion share of the heating power, and hence increased ion heat flux, facilitates the direct access to a sustained H-mode without entering in a dithering phase.

The T-NBI is a dominant electron heater, and behaves very differently to NBI or ICRH in deuterium and hydrogen plasmas, which are dominantly heated via the ions. Thus, the tendency of T-NBI and ICRH schemes in tritium plasmas favouring electron heating might explain the relatively higher power thresholds in terms of P_{sep} compared with the isotope dependent ITPA scaling reduced by 40% (grey line in figure 6, right).

In addition to the heating processes, which are taken into account by PION and PENCIL, it is possible that further effects can take place like incomplete absorption of ICRH power or direct losses of the fast tail of the ICRF heated species, which can reach the wall and increase the level of radiation [23]. This could be relevant for H–T mixed plasmas heated with a 2nd harmonic scheme, which has typically a lower absorption than fundamental heating especially in relatively cold plasmas as used for L–H transition studies.

5. Discussion

The presented results are mostly in agreement with the following possible physical processes, which determine P_{LH}, based on three ingredients:

(a) The L–H transition occurs when a critical edge ion heat flux is achieved. The critical ion heat flux depends, among

other factors like density, magnetic field and plasma surface, inversely on the isotope mass as described in reference [43]. This edge ion heat flux scaling is related to the (yet unknown but reproducible) *intrinsic* isotope dependence of the L–H transition.

(b) On top of this intrinsic effect, the pecularities of the heating scheme comes into play: the fraction of the input heating power, which arrives at the bulk ions, can effectively contribute to the increase of the edge ion heat flux up to the critical values necessary for the L–H transition. However, the power to electrons contributes only indirectly by equipartition and, thus, by a potentially much lower extent to the edge ion heat flux. The more off-axis the power is deposited to the electrons, the lower is the relative amount of equipartition due to competing transport processes. In other words, electron heating contributes much less to achieve an L–H transition.

(c) The radiation losses, P_{rad}, increase the total power, P_{loss}, necessary for the L–H transition. The radiated power can amplify the deleterious effect of electron heating, if the electrons are cooled before they can transfer their energy to the ions by equipartition.

Let us first discuss the P_{sep} data (figure 5, right), which should reveal effects of (a) and (b) independent of (c), since the radiation is subtracted in P_{sep}. The fact that the power to ion graph (figure 8, left) looks qualitatively similar to the graph of the P_{sep} data (figure 5, right), indicates that the power threshold P_{sep} behaves qualitatively like the expected intrinsic isotope dependence of the edge ion heat flux (a) with only minor corrections due to (b).

Furthermore, the power to ion data for the H–T mixed plasmas (figure 8, left) decreases monotonically with higher tritium concentration in agreement with the intrinsic isotope effect. Therefore, the expected isotope dependence is in general represented very well in the P_{sep} data, which might be given by the underlying intrinsic power threshold effect (a).

The small but systematically higher P_{sep} found in ICRF and T-NBI heated tritium plasmas with respect to the scaling might be attributed to the fact that the applied heating schemes are dominantly heating the electrons, thus, making it more difficult to reach the necessary critical ion heat flux. This indicates that effects of (b) are small but observable.

For engineering purposes, the more relevant power threshold quantity is P_{loss}. This can suffer from both a high power fraction of electron heating and high levels of radiation. P_{loss} is highest for hydrogen data due to the high intrinsic power threshold (a). Tritium has the lowest intrinsic power threshold (a) as it is obvious from the Ohmic and T-NBI data, but this advantage is compensated in ICRF heated tritium plasmas by the highest radiation contributions (c) of all isotopes and the tendency to high electron heating fractions (b).

The T-NBI tritium plasmas feature low levels of P_{rad}, hence, the corresponding data points of P_{loss} are very close to the isotope dependent ITPA scaling for metallic walls although they are dominantly electron heated. This demonstrates that the radiation effect (c) has a stronger impact on P_{loss} than the heating pecularities (b).

Obviously, although the Ohmic plasmas are predominantly electron heated plasmas, the electron–ion energy transfer is sufficient to develop an edge ion heat flux necessary to reach the L–H transition. This takes place despite the fact that the electron–ion transfer in T is lower than in D or H due to the higher mass ratio between tritium ions and electrons. However, the Ohmic plasmas have high energy confinement times, τ_E, exhibit low radiation and are comparably cold supporting sufficient electron–ion energy transfer. If our interpretation of the data in terms of our three steps (a) to (c) is correct, the data from Ohmic plasmas suggests that the intrinsic necessary edge ion heat flux in tritium is very low for low density.

6. Conclusion

The first study of the L–H power threshold, P_{LH}, in Ohmically, ICRF and T-NBI heated tritium plasmas in JET with ILW at a magnetic field of $B = 1.8$ T and a plasma current of $I_p = 1.7$ MA documents a clear isotope mass dependence of $P_{LH} \propto A_{eff}^{-1}$. This is in agreement with the JET results in a carbon wall [10], which suggested the same isotope dependence and which is in line with the general observations made in isotope studies at other fusion experiments [8, 11, 13, 22].

However, the power threshold in terms of P_{loss} of ICRF heated plasmas is much higher than in Ohmically or T-NBI heated tritium plasmas and up to a factor of two higher than the suggested isotope scaling for metallic wall machines, $P_{scal,ILW}$ (equation (8)). The undesired ICRF antenna phase setting present in most of the reported ICRH tritium pulses probably caused these higher radiation levels. In addition, the more effective sputtering of Be and W by T [39], and, thus, higher impurity levels, might likewise contribute to the elevated radiation levels in these pulses.

When the radiated power, P_{rad}, is taken into account for the ICRF heated tritium plasmas, the resulting L–H power threshold in terms of P_{sep} is on the same level as the T-NBI

heated pulses, but still slightly higher than the power threshold in Ohmic plasmas. This remaining trend of higher P_{sep} for ICRF and T-NBI heated plasmas with respect to that scaling, which describes best the hydrogen and deuterium data (isotope dependent ITPA scaling reduced by 40%), might be related to the fact that the heating schemes applied in tritium plasmas tend to dominantly heat the electrons.

A first analysis accounting for the effect of radiation and the pecularities of the heating schemes, which is based on assumptions due to the lack of ion temperature measurements, suggests that the JET-ILW data of P_{LH} is not inconsistent with the concept of a critical edge ion heat flux suggested by Ryter *et al* [21], further developed by Bilato *et al* [43] and applied for the design of pulses in ITER [1]. However, this has to be further investigated in more detail in the coming T and D–T campaigns, for which a much more accurate analysis due to the availability of ion temperature measurements is expected.

The implication of our results for future tritium containing plasmas as used in ITER or any D–T based classical tokamak is twofold. On the one hand, we confirmed the expected and favourable isotope scaling $P_{loss} \propto A_{eff}^{-1}$ in Ohmic and T-NBI heated plasmas for metallic wall machines, which raises hope that P_{LH} is comparably low in tritium, and that we can use this simple isotope scaling for predictions of P_{LH} in reactor relevant plasmas. On the other hand, the results clearly show that tritium plasmas can suffer significantly from high radiation and from dominant electron heating, which both tends to increase P_{LH} considerably. This is particularly the case in ICRF heated plasmas, but can also matter in general in reactor relevant plasmas, which tend to have higher radiation fractions for power exhaust purposes and higher electron heating fractions than present fusion devices. Thus, quantitative predictions of P_{LH} must take into account the effect of radiation and the pecularities of the heating schemes.

ORCID iDs

G. Birkenmeier https://orcid.org/0000-0001-7508-3646
E.R. Solano https://orcid.org/0000-0002-4815-3407
D. Taylor https://orcid.org/0000-0002-0465-2466
D. Gallart https://orcid.org/0000-0003-1663-3550
M.J. Mantsinen https://orcid.org/0000-0001-9927-835X

E. Delabie https://orcid.org/0000-0001-9834-874X
I.S. Carvalho https://orcid.org/0000-0002-2458-8377
P. Carvalho https://orcid.org/0000-0002-8480-0499
E. Pawelec https://orcid.org/0000-0003-1333-6331
F. Parra Diaz https://orcid.org/0000-0001-9621-7404
C. Silva https://orcid.org/0000-0001-6348-0505
S. Aleiferis https://orcid.org/0000-0001-7529-470X
J. Bernardo https://orcid.org/0000-0002-8197-7432
A. Boboc https://orcid.org/0000-0001-8841-3309
C.F. Maggi https://orcid.org/0000-0001-7208-2613
S.A. Silburn https://orcid.org/0000-0002-3111-5113

References

[1] ITER Organization 2018 ITER research plan within staged approach *ITR-Report 18-003* (https://iter.org/doc/www/content/com/Lists/ITER%2520Technical%2520Reports/Attachments/9/ITER-Research-Plan_final_ITR_FINAL-Cover_High-Res.pdf)

[2] Martin Y.R. and Takizuka T. (the ITPA CDBM H-mode Threshold Data Group) 2008 *J. Phys.: Conf. Ser.* **123** 012033

[3] Ryter F. *et al* 2013 *Nucl. Fusion* **53** 113003

[4] Chen L. *et al* 2016 *Nucl. Fusion* **56** 056013

[5] Hubbard A.E., Boivin R.L., Drake J.F., Greenwald M., In Y., Irby J.H., Rogers B.N. and Snipes J.A. 1998 *Plasma Phys. Control. Fusion* **40** 689

[6] Fukuda T. *et al* 1997 *Nucl. Fusion* **37** 1199

[7] Zhong W.L. *et al* 2020 *Nucl. Fusion* **60** 082002

[8] Gohil P., Evans T.E., Fenstermacher M.E., Ferron J.R., Osborne T.H., Park J.M., Schmitz O., Scoville J.T. and Unterberg E.A. 2011 *Nucl. Fusion* **51** 103020

[9] Andrew Y. *et al* (JET-EFDA contributors) 2006 *Plasma Phys. Control. Fusion* **48** 479

[10] Righi E. *et al* 1999 *Nucl. Fusion* **39** 309

[11] Ryter F. *et al* 2016 *Plasma Phys. Control. Fusion* **58** 014007

[12] Plank U. *et al* (ASDEX Upgrade Team) 2020 *Nucl. Fusion* **60** 074001

[13] Shao L.M. *et al* 2021 *Nucl. Fusion* **61** 016010

[14] Hillesheim J. *et al* 2016 Implications of JET-ILW L–H transition studies for ITER *2016 IAEA Fusion Energy Conf.* (Kyoto) EX/pp 5–2 (https://nucleus.iaea.org/sites/fusionportal/Shared%20Documents/FEC%202018/fec2018-preprints/preprint0346.pdf)

[15] Gohil P., Jernigan T.C., Osborne T.H., Scoville J.T. and Strait E.J. 2010 *Nucl. Fusion* **50** 064011

[16] Bourdelle C. *et al* 2014 *Nucl. Fusion* **54** 022001

[17] Andrew Y. *et al* 2008 *Plasma Phys. Control. Fusion* **50** 124053

[18] Field A.R. *et al* (the MAST Team) 2004 *Plasma Phys. Control. Fusion* **46** 981–1007

[19] Loarte A. *et al* 2021 *Nucl. Fusion* **61** 076012

[20] Wenninger R. *et al* 2017 *Nucl. Fusion* **57** 016011

[21] Ryter F., Barrera Orte L., Kurzan B., McDermott R.M., Tardini G., Viezzer E., Bernert M. and Fischer R. 2014 *Nucl. Fusion* **54** 083003

[22] Maggi C.F. *et al* 2018 *Plasma Phys. Control. Fusion* **60** 014045

[23] Lerche E. *et al* 2015 *AIP Conf. Proc.* **1689** 040003

[24] Van Eester D. and Koch R. 1999 *Plasma Phys. Control. Fusion* **40** 1949

[25] Kruezi U., Jepu I., Sergienko G., Klepper C.C., Delabie E., Vartanian S. and Widdowson A. 2020 *J. Instrum.* **15** C01032

[26] Vartanian S. *et al* 2021 *Fusion Eng. Des.* **170** 112511

[27] Solano E.R. *et al* 2017 *Nucl. Fusion* **57** 022021

[28] Réfy D.I. *et al* 2020 *Nucl. Fusion* **60** 056004

[29] Birkenmeier G. *et al* 2016 *Nucl. Fusion* **56** 086009

[30] Schmidtmayr M. *et al* 2018 *Nucl. Fusion* **58** 056003

[31] Maggi C.F. *et al* 2014 *Nucl. Fusion* **54** 023007

[32] Huber A. *et al* 2007 *J. Nucl. Mater.* **363–365** 365

[33] Ingesson L.C. 1997 Comparison of methods to determine the total radiated power in JET *JET Report JET-R(99)06* JET Joint Undertaking (https://scipub.euro-fusion.org/wp-content/uploads/2014/11/JETR99006.pdf)

[34] Ryter F. *et al* 1994 *Plasma Phys. Control. Fusion* **36** A99

[35] Martin Y.R. *et al* 2003 *Plasma Phys. Control. Fusion* **45** A351–65

[36] Fielding S.J., Ashall J.D., Carolan P.G., Colton A., Gates D., Hugill J., Morris A.W. and Valovic M. (the COMPASS-D, ECRH Teams) 1996 *Plasma Phys. Control. Fusion* **38** 1091

[37] Snipes J.A. *et al* 1994 *Nucl. Fusion* **34** 1039

[38] Huber A. *et al* 2021 *Phys. Scr.* **96** 124046

[39] Guillemaut C. *et al* 2016 *Phys. Scr.* **T167** 014005

[40] Lerche E. *et al* 2016 *Nucl. Fusion* **56** 036022

[41] Solano E.R. *et al* 2022 *Nucl. Fusion* **62** (076026

[42] Cavedon M. *et al* 2020 *Nucl. Fusion* **60** 066026

[43] Bilato R., Angioni C., Birkenmeier G. and Ryter F. (ASDEX Upgrade Team) 2020 *Nucl. Fusion* **60** 124003

[44] Vincenzi P. *et al* 2021 Power balance analysis at the L–H transition in JET-ILW NBI-heated deuterium plasmas *Plasma Phys. Control. Fusion* (accepted)

[45] Silva C. *et al* (JET Contributors) 2021 *Nucl. Fusion* **61** 126006

[46] Eriksson L.-G. and Hellsten T. 1995 *Phys. Scr.* **52** 70–9

[47] Challis C.D., Cordey J.G., Hamnén H., Stubberfield P.M., Christiansen J.P., Lazzaro E., Muir D.G., Stork D. and Thompson E. 1989 *Nucl. Fusion* **29** 563